EFFECTIVENESS OF FRICTION FORCE REDUCTION IN SLIDING MOTION DEPENDING ON THE FREQUENCY OF LONGITUDINAL TANGENTIAL VIBRATIONS, SLIDING VELOCITY AND NORMAL PRESSURE

Mariusz LEUS*, Paweł GUTOWSKI*, Marta RYBKIEWICZ*

*Faculty of Mechanical Engineering and Mechatronics, West Pomeranian University of Technology in Szczecin, al. Piastów 19, 70-310 Szczecin, Poland

mariusz.leus@zut.edu.pl, pawel.gutowski@zut.edu.pl, marta.rybkiewicz@zut.edu.pl

received 1 December 2022, revised 12 April 2023, accepted 4 May 2023

Abstract: The article presents the results of experimental research and simulation analyses of the influence of slip velocity, normal pressures and vibration frequency on the effectiveness of friction force reduction carried out in sliding motion in the presence of forced tangential vibrations. In experimental studies, changes in the driving force were measured during the slip of the upper body over the vibrating lower body. The direction of these vibrations was parallel both to the contact plane and to the direction of movement of the shifted body. The simulation tests were carried out in the Matlab/Simulink environment through the use of numerical procedures that were specially created for this purpose. Dynamic friction models considering the tangential compliance of contact and the phenomenon of pre-sliding displacement were used for calculations. The paper presents the designated values of the so-called coefficient of average friction force reduction in sliding motion for the following friction pairs: steel C45–steel C45, steel C45–cast iron GGG40 and steel C45–polytetrafluoroethy-lene PTFE (Teflon). The results of numerical analyses were in good agreement with those of experimental tests. A significant dependence of the level of average friction force reduction on the frequency of forced vibrations, sliding velocity as well as the kind of sliding pair material, and normal pressures was shown.

Key words: reduction of friction force, vibrations, experimental verification

1. INTRODUCTION

Due to the frequent need to minimise the force necessary to introduce a body into sliding motion and maintain this movement, the phenomenon of reducing the friction force has been and still is the subject of interest among scientists in many research centres around the world. The authors' own studies [1–8] and the works of other authors [9–24] indicate that introducing the shifted body or the substrate on which the slip takes place into a vibrating motion in a direction tangential to the track can significantly reduce the driving force, F_d. This phenomenon is identified with the reduction of the average friction force, $\bar{F}_f$ [19]. The level of this reduction depends on many factors related to the vibration parameters, sliding velocity and magnitude of surface pressures, as well as the kind of material and the microgeometry of contact surfaces of elements forming the sliding pair.

The direction of these vibrations in relation to the direction of slip is also an important factor, responsible for influencing to a large extent the effectiveness of the friction force reduction in the presence of forced vibrations. Different mechanisms of friction force reduction occur for vibrations normal to the contact plane [20, 24–31], and the ones occurring for tangential vibrations are different [1–24]. There are also two different friction force reduction mechanisms within tangential vibrations. Different for longitudinal vibrations – consistent with the direction of slip [2, 4–24], and different for transverse vibrations – perpendicular to this direction [1–3, 12, 19–24].

A condensed review of experimental works and model analyses related to the impact of tangential vibrations on friction processes in sliding motion is presented in the work of Shao et al. [25], as well as in several previous works of the authors of the present study [1–8]. This review shows that the greatest effectiveness of friction force reduction in tangential vibrations is possible when the direction of these vibrations is consistent with the direction of the macroscopic movement of the body being moved, i.e. in the case of longitudinal tangential vibrations. However, for the reduction of the friction force during longitudinal vibrations to occur, the amplitude of the vibration velocity v_a must be greater than the sliding velocity v_d. If this condition is not met, the reduction of the friction force will not occur during longitudinal vibrations.

It should be emphasised that, according to the results of the analyses presented in the study of Gutowski and Leus [4], reduction of the driving force in the sliding motion in the presence of tangential longitudinal vibrations, identified with the reduction of the average friction force, may occur both with temporary changes in the sign of the friction force and without such changes.

The fulfilment of the condition $v_a > v_d$ and the knowledge of the ratio v_a/v_d are not, however, tantamount to determining the level of friction force reduction under the influence of vibrations. In harmonic motion, the amplitude v_a of vibration velocity is a function of two independent vibration parameters, which determine the level of friction force reduction. It is a function of both the frequency f of the vibrations and the amplitude u_o of their displacements.

Thus, the reduction level cannot be unequivocally determined only on the basis of the value of vibration velocity amplitude since the same value of this parameter can be obtained at different values of frequency and amplitude of vibrations. Hence, an important information in the studies of sliding motion in the presence of forced longitudinal tangential vibrations is not only the knowledge of the individual influence that each of these vibration parameters exert on the level of friction force reduction but also the knowledge of their cumulative influence on this reduction. It shows that, in all analyses of the impact of vibrations on the friction force in sliding motion and in particular when using these vibrations to control the friction force on the contact surfaces of the friction pair, both vibration parameters u_o and f must be considered. Maintaining the amplitude v_a of vibration velocity at a constant level does not mean the maintenance of a constant level of friction force reduction.

The available literature lacks both model and experimental analyses illustrating this very important, especially due to the possibility of practical use, impact of the simultaneous change of both vibration parameters, i.e. their frequency f and displacement amplitude u_o, on the level of friction force reduction in sliding motion. Hence, the purpose of this work was to fill this prevalent gap in the existing literature.

This work considers the experimental and numerical analyses of the influence of the sliding velocity, normal pressures and the frequency of forced vibrations on the effectiveness of friction force reduction in sliding motion performed in the presence of longitudinal tangential vibrations. Simulation studies of the friction force reduction as a function of these parameters were carried out in the Matlab/Simulink environment, using the computational model described in detail in the study of Gutowski and Leus [4]. Two relatively simple, dynamic friction models were used there to describe the friction force: the Dahl model [32, 33] and the elasto-plastic model [34, 35]. In the Dahl model, it is assumed that the contact deformations in the tangential direction are elastoplastic already from the initial load phase. In the second of these adopted friction models, there is a pure-elastic phase before the elasto-plastic deformation phase. In these models, the friction force F_f is a function of contact tangential stiffness, the measure of which is the coefficient k_t, and depends on the magnitude of the elastic deformation s of the contact area ($F_f = k_t \cdot s$) [32–35]. It is evident that assuming the wrong value of the coefficient k_t will lead to incorrect determination of the level of friction force reduction. The values of this coefficient, for a given set of contact joints of sliding pairs tested in this paper, were determined experimentally from the compliance characteristics of these joints plotted in the tangential direction. The appropriate tests were carried out on the tests stand described in the study of Leus and Gutowski [36].

The experimental tests of the friction force reduction as a function of the frequency of forced vibrations, sliding velocity and normal pressures presented in this article were carried out, in turn, on the test stand described in work [2].

The present study provides the experimentally and numerically determined values of the coefficient of average friction force reduction at a fixed amplitude u_o of vibrations (u_o = const) and changing values of the frequency f of these vibrations, for different drive velocities v_d and strictly defined normal pressures p. Experimental and simulation tests were carried out for three sliding pairs, namely steel C45–steel C45, steel C45–cast iron GGG40 and steel C45–polytetrafluoroethylene PTFE (Teflon).

Introducing vibrations of a set amplitude and frequency into the contact area of the shifted body and the ground is not always possible due to hardware limitations, such as limited power of the vibration exciter, and often, it may even be unacceptable because of the resonance phenomenon. Hence, the paper also presents the results of model and experimental analyses of changes in the level of friction force reduction under the influence of vibrations, with simultaneous modification of both the frequency f and the amplitude u_o of vibrations. These changes in the values of vibration parameters were made in such a way that the ability to reduce the friction force by means of introduced longitudinal vibrations is maintained, resulting from the necessary fulfilment of the condition $v_a > v_d$. These tests were carried out at a fixed value of the velocity amplitude v_a = const, meeting this condition.

2. EXPERIMENTAL INVESTIGATIONS

The experimental tests were carried out on the test stand that is shown in Fig. 1. A complete description of this test stand is included in the study of Gutowski and Leus [2]. Its main part is a sliding pair consisting of specially designed specimens: upper A and lower B. During tests, the upper specimen is shifted with a set velocity over the lower specimen by means of a drive system consisting of a stepper motor with a gear, a linear guide and a driver. In the initial stage of this shift, the lower specimen is fixed, and then, while the upper specimen is moving, it is set into vibration motion generated by a piezoelectric vibration actuator. At the final stage of the test, the vibration generator is turned off, and the upper sample is moved again over the stationary lower specimen. Each experimental test at each measurement point was repeated thrice.

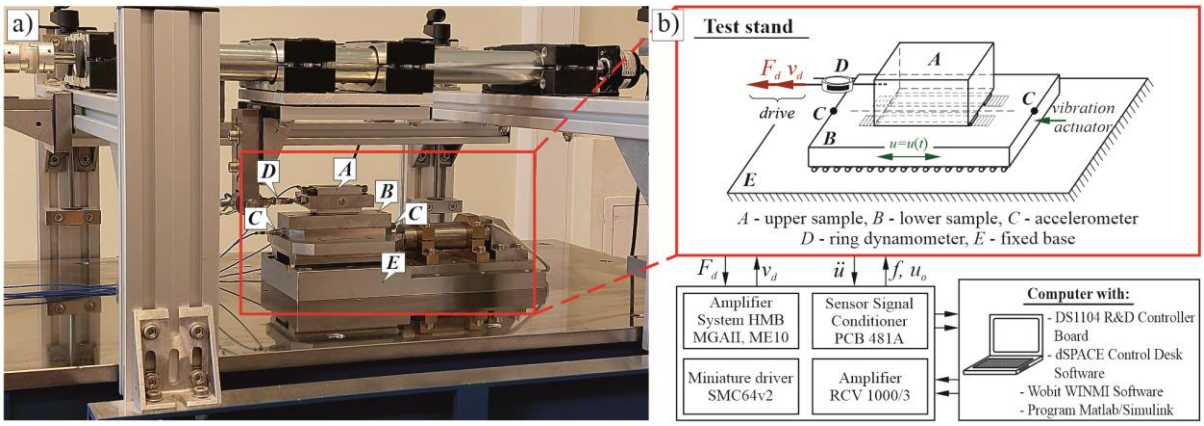

Fig. 1. Test stand: (a) photo of the mechanical part of the stand prepared for testing and (b) block diagram of the measurement and data handling system

The tests were carried out with harmonic forcing of the lower specimen. Its displacement was described by the relationship:

$$u = u_o \sin(\omega t) \tag{1}$$

where u_o is vibration amplitude, ω is angular frequency of vibrations ($\omega = 2\pi f$) and f is vibration frequency.

The vibration velocity of the lower specimen was given by the following expression:

$$\dot{u} = v_a \cos(\omega t) \tag{2}$$

where v_a is an amplitude of vibration velocity. It is a function of both the frequency f and the amplitude u_o of the vibrations:

$$v_a = u_o \omega = 2\pi f u_o \tag{3}$$

During the tests, throughout the shift of the upper specimen, the drive force necessary at first to set this specimen into sliding motion, and then to maintain this motion, was measured. This force was measured with a special ring dynamometer D (Fig. 1) placed between the upper specimen and the driver. The values set during the measurement were drive velocity v_d, frequency f and amplitude u_o of forced vibrations and surface pressures p. For control purposes, during each measurement, the acceleration of the lower specimen was also registered with the use of miniature acceleration sensors such as M352C65 type ICP (manufactured by PCB).

The contact pressure p, normal to the contact surface, is the result of the self-weight of the upper sample with an additional load of m_1 = 1 kg attached to it and the external force F_z applied to this sample centrally in the vertical direction, in concomitance with the use of a lever containing sliding weights for string loading [6]. Such a system allows us to obtain normal pressures on the contact surface of the friction pair starting from p_{min} = 0.00544 N/mm^2 up to p_{max} = 0.120 N/mm^2. The contact pressure, during the sliding/vibration interactions, was controlled continuously by means of a force gauge placed on the vertical string, connecting the sliding sample with the lever with sliding weights.

The surface roughness of the specimens, forming the tested contact joints (Fig. 2a–c), was measured with a profilometer (Mitutoyo Surftest SJ-210) (Fig. 2d). Tab. 1 shows the measured R_a values of the upper and lower specimens. Each of the values given in this table is an average of six surface roughness measurements carried out in different places of the contact surface. All measurements were performed in the direction of the slip.

Tab. 1. R_a parameters of sliding pair samples

Sample	Material	R_a [μm]	
		Mean	Stand. dev.
Upper	Steel C45	0.44	0.038
Lower	Steel C45	1.35	0.095
	Cast iron GGG40	1.14	0.099
	PTFE	2.05	0.246

PTFE, polytetrafluoroethylene

Experimental tests were carried out in normal room conditions at temperatures ranging from 22° to 26°C. Ambient humidity was not measured.

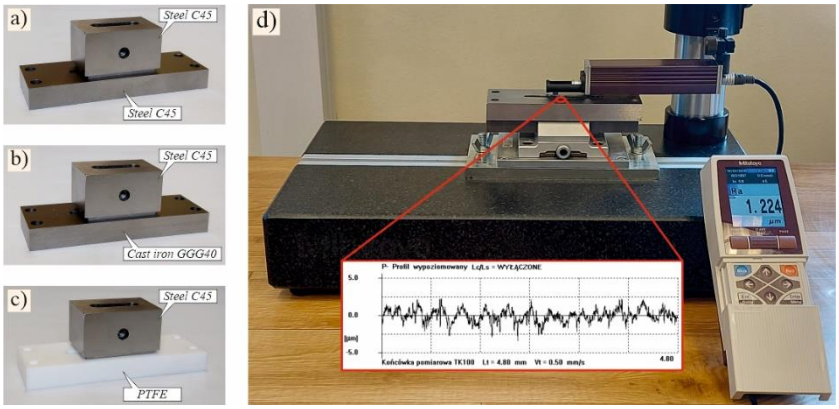

Fig. 2. Photos of specimens prepared for testing and roughness measurement stand: (a) steel–steel, (b) steel–cast iron, (c) steel–PTFE and (d) profilometer Mitutoyo Surftest SJ-210

For each sliding pair, during the measurements, the change in the driving force F_d was measured as a function of the vibration frequency f at the determined amplitude u_o = 0.1 μm. The tests were carried out at five different frequencies f of forced vibrations, namely 1 kHz, 2 kHz, 3 kHz, 4 kHz and 5 kHz, with vibration velocity amplitudes of v_a = 0.628 mm/s, 1.256 mm/s, 1.884 mm/s, 2.513 mm/s and 3.141 mm/s, respectively; and for four drive velocities, v_d = 0.2 mm/s, 0.5 mm/s, 1 mm/s and 2 mm/s. These measurements were performed for three selected values of normal pressures: p = 0.022 N/mm^2, 0.063 N/mm^2 and 0.104 N/mm^2. Examples of test results in the form of drive force plots for the analysed friction pairs at v_d = 0.5 mm/s and p = 0.063 N/mm^2 are shown in Fig. 3.

The comparison of the driving force runs shown in Figure 3 indicates that, in all the presented cases, the introduction of longitudinal vibrations into the contact area of the friction pair resulted in a decrease in the driving force necessary to maintain the sliding movement of the upper sample. The higher the frequency f of the forced vibrations, the greater was the magnitude of this reduction, which means that it increased with the increase of the amplitude of the vibration velocity v_a, because with a fixed displacement amplitude u_o, the increase in the frequency of vibrations causes a corresponding increase in the amplitude of the vibration velocity. From the runs shown in Fig. 3, it can also be seen that the level of this reduction depends on the type of friction pair, and it was the lowest in the case of the steel C45–PTFE pair.

It should be emphasised that in any tests carried out with forced vibrations of the ground with amplitudes of velocity v_a lower than the drive velocity v_d, there was no reduction of the driving force.

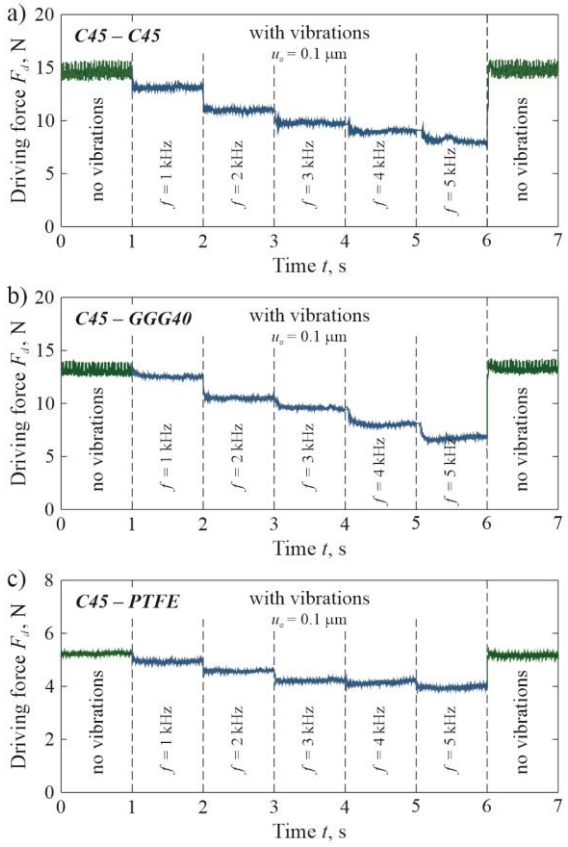

Fig. 3. Variability of the driving force F_d in relation to frequency f at fixed amplitude u_o of vibration: (a) steel–steel, (b) steel–cast iron and (c) steel–PTFE; p = 0.063 N/mm², v_d = 0.5 mm/s, u_o = 0.1 μm

3. SIMULATION ANALYSES AND THEIR EXPERIMENTAL VERIFICATION

Numerical studies were carried out using the model developed to analyse the effect of longitudinal tangential vibrations on the friction force in sliding motion, as described in detail in the study of Gutowski and Leus [4]. This model is based on the dynamic equation of motion of a body sliding over the ground, which is introduced into vibrations in a strictly defined direction, i.e. a direction parallel to both the contact plane and the direction of the sliding body motion. To describe the friction force, dynamic friction models such as the Dahl model [32, 33] and the elastoplastic [34, 35] model were adopted. The simulation tests were carried out in the Matlab/Simulink environment in accordance with the calculation algorithm presented in Fig. 4.

The main purpose of the model simulation analyses was, as in the experimental studies, to examine the impact of the frequency of tangential longitudinal vibrations, as well as the sliding speed and surface pressures, on the level of friction force reduction in sliding motion. The comparison of the obtained results of model analyses with the results of experimental tests also allowed us to assess the correctness of the developed calculation procedures.

The analyses were carried out at the forced vibration frequencies f of the lower specimen ranging from 0 kHz to 6 kHz. The drive velocity v_d and normal pressures p in the contact area of the upper and lower specimens were identical to those in the experimental tests. The value of the contact stiffness coefficient k_t of the analysed sliding pair contact, at given pressure p, was determined based on curves $k_t = f(p)$ described by equations given in Tab. 2. These relationships were determined experimentally for the tested sliding pairs in the range of normal pressures from p = 0.014 N/mm² to p = 0.112 N/mm², in accordance with the procedures presented in the study of Leus and Gutowski [36].

Tab. 2. Regression equations and the values of curves $k_t = f(p)$ correlation coefficient R^2 for given sliding pairs

Sliding pair	Regression equation, $k_t = f(p)$	Correlation coefficient R^2
C45–C45	$k_t = 917.36p^2 + 289.22p + 55.663$	0.9899
C45–GGG40	$k_t = 4089.9p^2 + 186.42p + 44.116$	0.9955
C45–PTFE	$k_t = -57.381p^2 + 46.7p + 2.1792$	0.9891

Values of contact stiffness coefficients k_t of tested sliding pairs at normal pressures at which the simulation analyses have been performed are given in Table 3.

Tab. 3. Values of contact stiffness coefficients k_t of sliding pair contact at normal pressures p assumed in performed tests

Sliding pair	k_t [N/μm]		
	p = 0.022 [N/mm²]	p = 0.063 [N/mm²]	p = 0.112 [N/mm²]
C45–C45	62.47	77.52	95.66
C45–GGG40	50.20	72.15	107.74
C45–PTFE	3.18	4.89	6.42

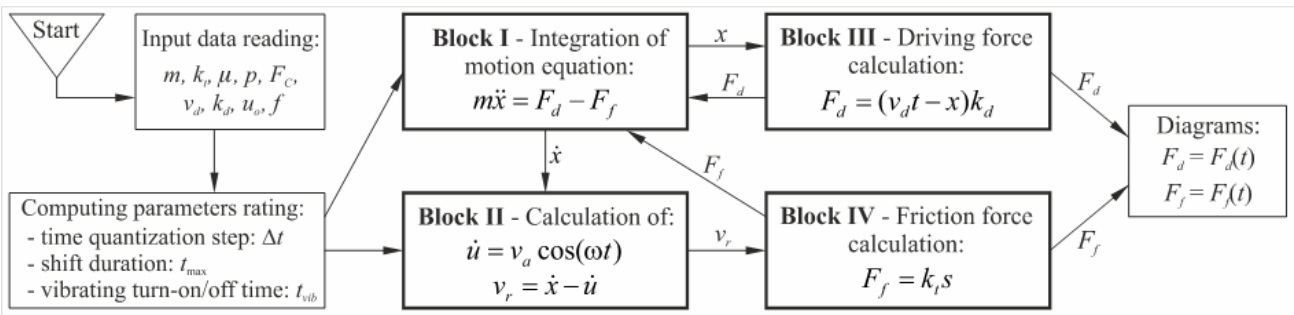

Fig. 4. Algorithm for calculating the friction force in sliding motion at longitudinal vibrations

In the simulation analyses, it was assumed that the stiffness of the drive system was k_d = 0.92 N/μm. This value was determined experimentally on the test stand as described in the study of Leus [5]. Moreover, it was assumed that the damping of the drive was negligible. Such an assumption was made because there were no sliding joints between the driver and the movable upper sample, in which the vibration energy could be dissipated, and all drive elements between the driver and this sample were steel elements with very low material damping. It was therefore assumed that the drive damping coefficient was h_d = 0.

It was also assumed that the mass of the sliding upper steel sample together with the additional weight attached to it was m = 1.665 kg and that the coefficients of friction of the tested sliding pairs were μ_1 = 0.193, μ_2 = 0.176 and μ_3 = 0.071, for the steel–steel pair, steel–cast iron pair and steel–PTFE pair, respectively. These values were determined on the same test stand on which the experimental tests of friction force reduction under the influence of vibrations, described in this paper, were carried out.

In the conducted simulation analyses, at each measurement point, the calculations were started with the upper sample immobile and the ground immobilised. Therefore, it was assumed that at the initial moment for the sliding sample, x_o = 0 and $\dot{x}$ = 0, and the amplitude of the ground vibrations at the initial moment was u_o = 0. The vibrations of the ground were excited for some time after the start of the sliding movement of the upper sample. In the simulation analyses described in the paper, this time was t = 0.04 s. The friction pair materials used in the experimental tests and adopted in the numerical analyses, such as C45 steel, GGG40 cast iron and PTFE, can be classified as ductile materials. Therefore, the shape factor α in the Dahl model and in the elastoplastic model for these materials, according to the data contained in the study of Dahl [33], must meet the condition $\alpha \geq 1$. In this paper, in simulation analyses, the value α = 1 was assumed.

To evaluate the effectiveness of the friction force reduction, the dimensionless value of parameter ρ was adopted and described by the following relationship:

$$\rho = \frac{\bar{F}_f}{F_C} \tag{4}$$

where $\bar{F}_f$ is an average friction force in the contact of a given friction pair during one period of vibrations, corresponding to the value of drive force F_d necessary to introduce the body into sliding motion and maintain this motion, with set vibration parameters f and u_o, drive velocity v_d and normal pressures p, while F_C is the Coulomb friction force, i.e. the friction force without vibrations.

The average value $\bar{F}_f$ of the friction force during one vibrations period T can be determined in numerical analyses from the following relationship:

$$\bar{F}_f = \frac{1}{n}\sum_{i=1}^{n} F_f(t + i\Delta t) \tag{5}$$

where n is the number of time steps Δt into which one period T of vibrations was divided.

The value ρ = 1 means no reduction of friction force, while when ρ < 1, the reduction takes place. The smaller the value of parameter ρ, the greater the reduction of friction force.

Figs. 5 and 6 summarise the results of simulation studies and the corresponding results of experimental tests in the form of collective diagrams. These figures present plots of variations of the parameter ρ as a function of forced vibrations frequency f for four fixed drive velocities, namely 0.2 mm/s, 0.5 mm/s, 1 mm/s and 2 mm/s. Numerical waveforms are marked with lines, while the results of experimental tests are marked with points. Fig. 5 presents the results obtained for the sliding steel–steel pair for three values of normal pressures, namely p = 0.022 N/mm², 0.063 N/mm² and 0.104 N/mm², while the results presented in Fig. 6 pertain to the analyses carried out for the sliding steel–cast iron pair (Fig. 6a) and the steel–PTFE pair (Fig. 6b). These analyses were performed at normal pressures, p = 0.063 N/mm².

The graphs presented in Figs. 5 and 6 show the average values of three measurement results together with marked standard deviations. It should be emphasised that very good repeatability of the results was obtained in subsequent repetitions. This is evidenced by the value of standard deviations, which for the most part did not exceed the level of 4% of the average value determined at a given measurement point. The very good repeatability of the results proves that the number of repetitions has no significant effect on the quality of conclusions regarding the nature of the studied phenomenon.

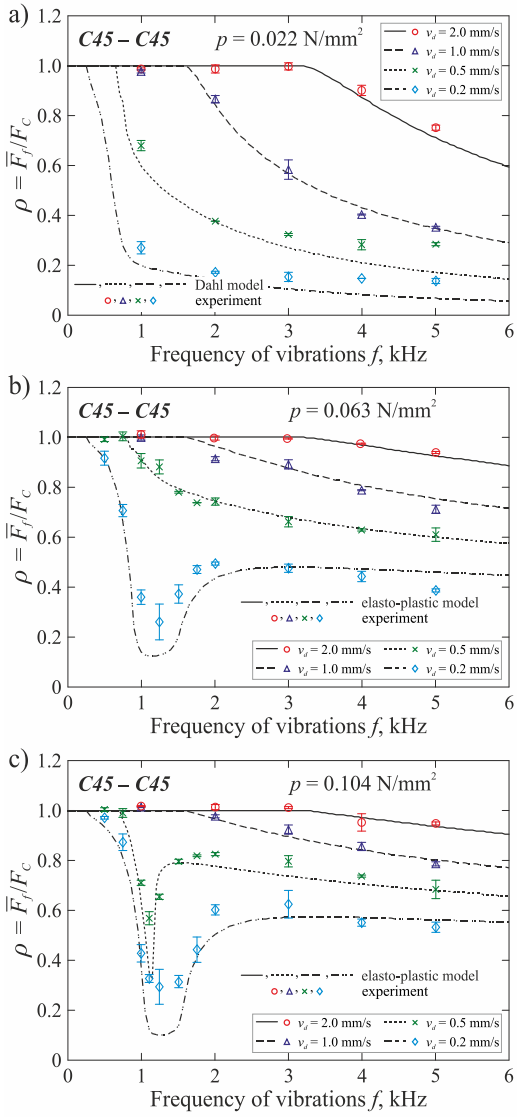

Fig. 5. Effectiveness of friction force reduction for joint steel–steel as a function of vibrations frequency f at their fixed amplitude u_o = 0.1 μm and different normal pressures: (a) p = 0.022 N/mm², (b) p = 0.063 N/mm² and (c) p = 0.104 N/mm²

The results of experimental tests and numerical analyses presented in Figs. 5 and 6 clearly indicate that, when the condition $v_a > v_d$ was not fulfilled, introducing longitudinal tangential vibrations into the contact area of the sliding body and the ground did not change the friction force. For the drive velocities adopted in the tests v_d = 2 mm/s, 1 mm/s, 0.5 mm/s and 0.2 mm/s, the boundary frequencies at the beginning of the friction force reduction at longitudinal vibrations with the amplitude u_o = 0.1 μm, according to Eq. (3), are 3183 Hz, 1591.5 Hz, 795.75 Hz and 318.3 Hz, respectively. The reduction occurred only in the case where $v_a > v_d$ and it was the higher, the higher was the frequency of forced vibrations f and the lower was the drive velocity v_d.

The comparison of the plots in Fig. 5 for the friction steel–steel pair indicates that the level of friction force reduction depends on the normal pressures p. These plots clearly show that with the increase in normal pressures on the contact surface, the value of the parameter ρ visibly increased, which means that the increase in normal pressures caused a lowering of the level of friction force reduction.

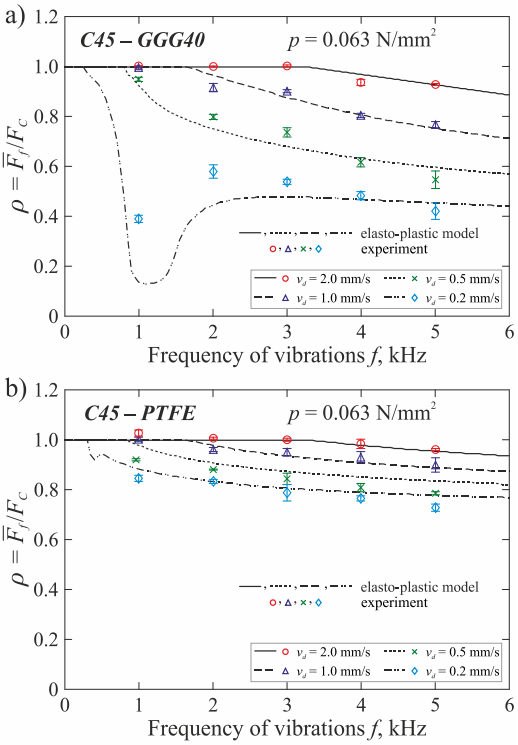

Fig. 6. Effectiveness of friction force reduction as a function of vibrations frequency f at their fixed amplitude u_o = 0.1 μm for joints: (a) steel–cast iron and (b) steel–PTFE; p = 0.063 N/mm²

In turn, when comparing the friction force reduction curves for different materials of friction pairs as presented in Figs. 5b, 6a and 6b, determined with the same vibration parameters u_o and f, the same pressures p and the same drive velocities v_d, it can be noticed that definitely the smallest of friction force reduction under the influence of longitudinal tangential vibrations occurs in the joint steel–PTFE pair. However, in the case of the two remaining friction pairs, i.e. steel–steel and steel–cast iron, the level of friction force reduction was definitely higher – the highest was for the steel–steel contact, while that for the steel–cast iron contact was only slightly less. In all three presented cases, the vibrations parameters, such as amplitude u_o and frequency f as well as drive velocity v_d and surface pressures p, were the same in tests. The frictional pairs differed in the kind of material of the lower specimen and the roughness of this sample's surface. Therefore, the tangential compliance of contact of these pairs was also different. At the pressure p = 0.063 N/mm², the stiffness coefficients k_t of the tested contacts, in accordance with the equations given in Tab. 3, were derived as k_t = 77.5 N/μm, k_t = 72.09 N/μm and k_t = 4.89 N/μm for steel–steel pair, steel–cast iron pair and steel–PTFE pair, respectively. It can be noticed that the tangential stiffness of the steel–PTFE contact was definitely lower than that of the other two contacts. Hence, a significantly lower level of friction force reduction was obtained in this contact as compared with the other two friction pairs. This result is consistent with the results of the study of Gutowski and Leus [4].

The results of friction force reduction obtained at low frequencies of 0.5–1.5 kHz and higher pressures p = 0.063 N/mm² (Fig. 5b and Fig. 6a) and p = 0.104 N/mm² (Fig. 5c) for steel – steel and steel – cast iron pairs that deviate from the clear trend require a separate comment. The reason for this happening was probably the fact that at these frequencies and these surface pressures, the phenomenon of resonance occurs for the shifted specimen.

To prove the appearance of this resonance from the numerical model developed in Matlab/Simulink, for the analysis of the impact of vibrations on the friction force, displacement diagrams of the upper sample being moved during the ground vibrations were generated. They were generated at various normal pressures p. These diagrams are shown in Fig. 7. They clearly indicate that at the assumed normal pressures, in the excitation frequency range of f = 500–1500 Hz, the system is subject to the phenomenon of resonance.

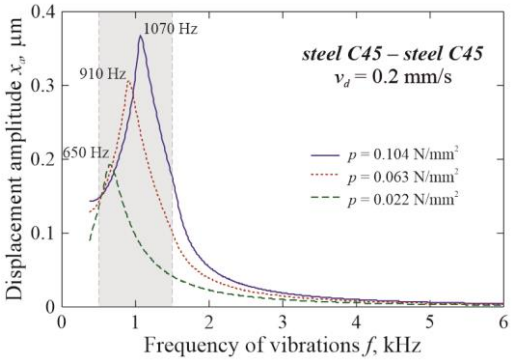

Fig. 7. Diagrams of the displacement of the upper sample on a vibrating ground, illustrating the occurrence of resonance in the frequency range f = 500–1500 Hz

4. REDUCTION OF FRICTION FORCE AT A FIXED AMPLITUDE OF VIBRATIONS VELOCITY

When analysing the influence of longitudinal tangential vibrations on the friction force in sliding motion, the most important parameter is the amplitude of the vibration velocity v_a, because its value determines the upper limit of the sliding velocity – the drive velocity – above which the reduction of the friction force does not occur. In harmonic motion, the value of this amplitude is determined based on dependence (3), which means that in real systems, it can be controlled by two vibration parameters: amplitude u_o and frequency f, which are changed simultaneously; or, one of them is at a fixed value with respect to the other parameter.

In this paper, this problem is illustrated by presenting the results of experimental and numerical tests of changes in the level

of friction force reduction at the amplitude of vibration velocity v_a fixed at the level that guarantees the occurrence of the friction force reduction, i.e. $v_a > v_d$, but with a different set of the vibration parameters u_o and f, while maintaining a constant value of vibration velocity amplitude, v_a = const. Here, v_a = 1.256 mm/s was assumed.

The tests were carried out for the same friction pairs as in the previous case, with five frequencies of forced vibrations f, namely 1 kHz, 2 kHz, 3 kHz, 4 kHz and 5 kHz, and for four drive velocities: v_d = 0.2 mm/s, 0.5 mm/s, 1 mm/s and 2 mm/s. In order to maintain a constant value of the vibration velocity amplitude, v_a = const, with each change of frequency f, the value of the amplitude u_o was changed suitably in accordance with the dependence (3). As before, these measurements were made at three selected values of normal pressure: p = 0.022 N/mm², 0.063 N/mm² and 0.104 N/mm². Examples of test results in the form of drive velocity plots for the analysed friction pairs at v_d = 0.5 mm/s and p = 0.063 N/mm² are presented in Fig. 8.

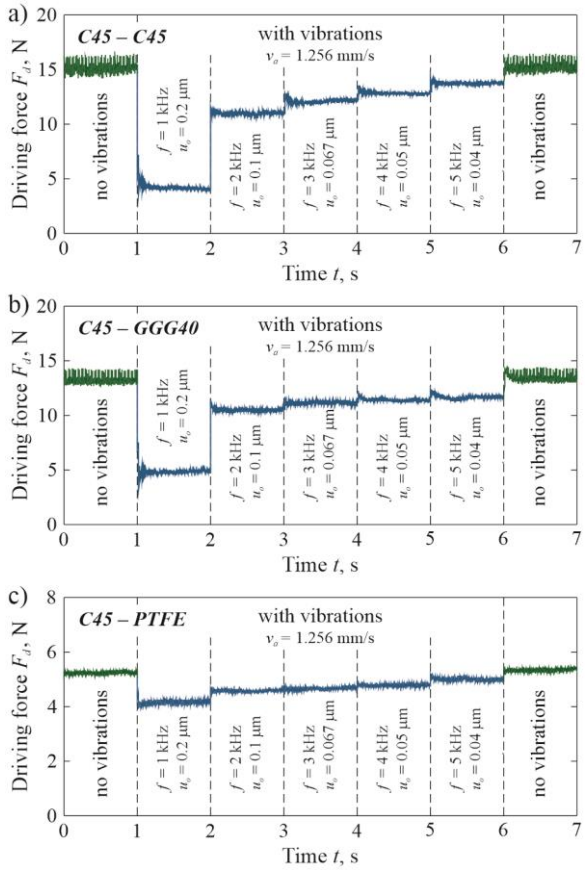

Fig. 8. Variability of the driving force F_d in relation to frequency f and amplitude u_o at fixed amplitude of vibration velocity v_a = const: (a) steel–steel, (b) steel–cast iron and (c) steel–PTFE; p = 0.063 N/mm², v_d = 0.5 mm/s, v_a = 1.256 mm/s

Figs. 9 and 10 present the results of simulation studies and the corresponding results of experimental tests in the form of collective plots. These figures show plots of changes of the parameter ρ as a function of increasing frequency f and correspondingly decreasing vibrations amplitude u_o at a fixed value of vibration velocity amplitude v_a = const for four drive velocities v_d, namely 0.2 mm/s, 0.5 mm/s, 1 mm/s and 2 mm/s. Numerical results are marked with lines, while the results of experimental tests are marked with points. Fig. 8 presents the results obtained for the sliding steel–steel pair for three values of normal pressures: p = 0.022 N/mm², 0.063 N/mm² and 0.104 N/mm². The results presented in Fig. 10 pertain to the analyses carried out for the sliding steel–cast iron pair (Fig. 10a) and for the steel–PTFE pair (Fig. 10b).

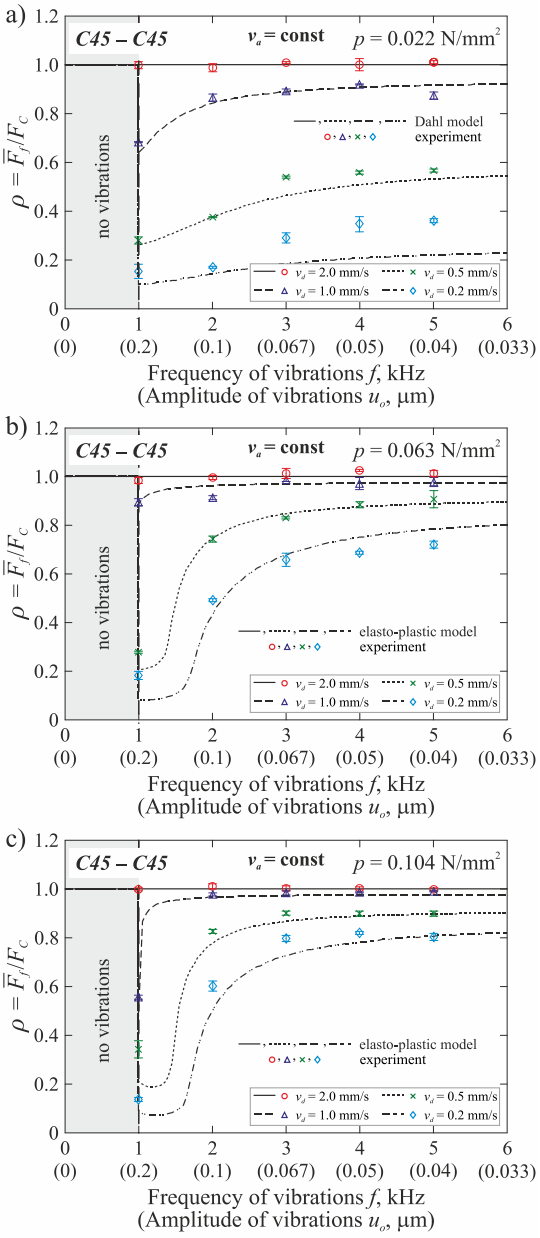

Fig. 9. Change of the reduction coefficient ρ at different pressures p and fixed vibrations velocity amplitude v_a = const caused by increasing the frequency f with a simultaneous reduction of vibrations amplitude u_o for the pair steel–steel: (a) p = 0.022 N/mm², (b) p = 0.063 N/mm², (c) p = 0.104 N/mm²; v_a = 1.256 mm/s

From the obtained results of the experimental tests and numerical analyses presented in Figs. 9 and 10, it can be noticed that when v_d = 2 mm/s, i.e. when the condition that $v_a > v_d$ was not fulfilled, the reduction of friction force did not occur in any of the considered cases. For the three remaining values of v_d = 1 mm/s, v_d = 0.5 mm/s and v_d = 0.2 mm/s, the excitation of vibrations caused a reduction of the friction force, which resulted in the

reduction of the parameter ρ to a value lower than 1. The effectiveness of this reduction is significantly influenced by the ratio of drive velocity v_d to vibration velocity amplitude v_a and excitation frequency f, the kind of material of the sliding pair and the value of normal pressures p in the plane of contact between the shifted body and the ground. The lower the drive velocity v_d relative to the amplitude v_a, the higher the reduction level.

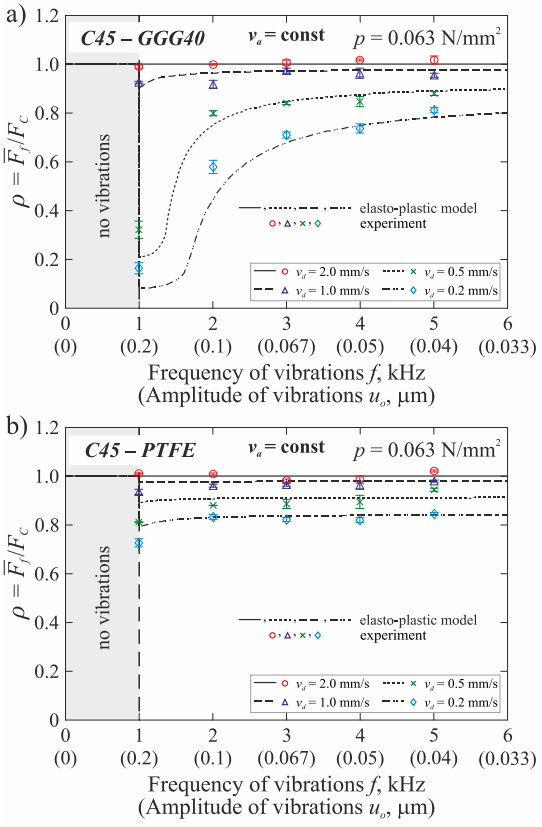

Fig. 10. Change of the reduction coefficient ρ at fixed vibration velocity amplitude v_a = const, caused by increasing the frequency f with a simultaneous reduction of vibrations amplitude u_o for the pair: (a) steel–cast iron and (b) steel–PTFE; p = 0.104 N/mm^2; v_a = 1.256 mm/s

Increasing the frequency of vibrations with a simultaneous reduction of their amplitude, in order to maintain a constant value of the vibrations velocity amplitude, resulted in an increase in the value of the parameter ρ in each of the analysed cases. This means that such a treatment reduces the level of friction force reduction under the influence of longitudinal vibrations introduced into the contact area. As in the previous test variant, the test results from this variant, presented in Figs. 9 and 10, clearly indicate that both the increase in normal pressures on the contact surface of friction pair and the increase in sliding velocity reduce the effectiveness of the friction force reduction.

5. CONCLUSIONS

The conducted simulation analyses and experimental tests demonstrate that the influence of the forced longitudinal tangential vibrations on the friction force in sliding motion is highly complex. These vibrations can cause an explicit reduction of the drive force necessary to start and maintain the slip of one body over another, but the necessary condition for this reduction to occur is that the vibration velocity amplitude v_a be higher than the drive velocity v_d. However, the value of the parameter v_a cannot be treated as a determinant of the reduction level, because, as shown by the conducted tests, with a constant vibration velocity amplitude v_a, different values of the frequency f and the amplitude u_o of these vibrations, as well as different reduction effectiveness values of the average friction force, can be obtained. The reason is that the amplitude of the vibration velocity is a function of both of the above-mentioned vibration parameters, i.e. their frequency and amplitude of displacement.

The conducted research clearly indicates that the increase in the vibrations frequency with their constant amplitude increases the effectiveness of the friction force reduction under the influence of longitudinal tangential vibrations, while the increase in surface pressure and the increase in drive velocity cause the opposite effect – lowering the level of reduction of this force. In an extreme case, a slip at a velocity higher than the vibration velocity amplitude eliminates the possibility of using longitudinal vibrations to achieve a reduction in friction force.

An important conclusion resulting from the conducted research is that with low contact stiffness, related to the kind of material of the elements forming the friction pair and higher roughness of the contact surfaces, the effect of friction force reduction under the influence of vibrations is visible lower than that obtained in case of contact with high stiffness, and furthermore, the level of this reduction depends to a much lesser extent on the frequency of the vibrations.

There is a very good agreement between the results of numerical calculations and experimental tests, even at resonant frequencies of the sliding pair, which proves the correctness of the developed procedures for the analyses of the effect of longitudinal tangential vibrations on the friction force in sliding motion and proves the possibility of using these procedures to control the friction force in the sliding motion of real objects by means of vibrations.

REFERENCES

1. Gutowski P, Leus M. Computational model for friction force estimation in sliding motion at transverse tangential vibrations of elastic contact support. Tribology International. 2015;90:455-462. https://doi.org/10.1016/j.triboint.2015.04.044
2. Gutowski P, Leus M. Computational model of friction force reduction at arbitrary direction of tangential vibrations and its experimental verification. Tribology International. 2020;143:106065. https://doi.org/10.1016/j.triboint.2019.106065
3. Gutowski P, Leus M. Estimation of the tangential transverse vibrations effect on the friction force with the use of LuGre model. Acta Mechanica. 2021;232(10):3849-3861. https://doi.org/10.1007/s00707-021-03033-1
4. Gutowski P, Leus M. The effect of longitudinal tangential vibrations on friction and driving forces in sliding motion. Tribology International. 2012;55:108-118. https://doi.org/10.1016/j.triboint.2012.05.023
5. Leus M. Investigation of the longitudinal tangential contact vibrations influence on the friction force. Doctoral thesis. 2010.
6. Leus M, Gutowski P. Practical possibilities of utilization of tangential longitudinal vibrations for controlling the friction force and reduction of drive force in sliding motion. Mechanics and Mechanical Engineering. 2011;15(4):103-113.
7. Rybkiewicz M, Gutowski P, Leus M. Experimental and numerical analysis of stick-slip suppression with the use of longitudinal tangential vibration. Journal of Theoretical and Applied Mechanics. 2020;58(3):637-648. https://doi.org/10.15632/jtam-pl/116594

8. Rybkiewicz M, Leus M. Selection of the friction model for numerical analyses of the impact of longitudinal vibration on stick-slip movement. Advances in Science and Technology Research Journal. 2021;15(3):277-287. https://doi.org/10.12913/22998624/141184
9. Gao H, De Volder M, Cheng T, Bao G, Reynaerts D. A pneumatic actuator based on vibration friction reduction with bending longitudinal vibration mode. Sensors and Actuators A: Physical. 2016;252:112-119. https://doi.org/10.1016/j.sna.2016.10.039
10. Kapelke S, Seemann W. On the effect of longitudinal vibrations on dry friction: Modelling aspects and experimental investigations. Tribology Letters. 2018;66(3):1-11. https://doi.org/10.1007/s11249-018-1031-0
11. Kapelke S, Seemann W, Hetzler H. The effect of longitudinal high-frequency in-plane vibrations on a 1-DoF friction oscillator with compliant contact. Nonlinear Dynamics. 2017;88:3003-3015. https://doi.org/10.1007/s11071-017-3428-y
12. Kumar VC, Hutchings IM. Reduction of sliding friction of metals by the application of longitudinal or transverse ultrasonic vibration. Tribology International. 2004;37(10):833-40. https://doi.org/10.1016/j.triboint.2004.05.003
13. Kutomi H, Sase N, Fujii H. Development of friction controller. Proceedings of the International Conf AMPT'99. 1999;I:605-612.
14. Littmann W, Stork H, Wallaschek J. Reduction of friction using piezoelectrically excited ultrasonic vibrations. Proceedings of the SPIE's 8th Annual International Symposium on Smart Structures and Material, Billingham, Washington 2001. 2001;302-311. https://doi.org/10.1117/12.432714
15. Littmann W, Stork H, Wallaschek J. Sliding friction in the presence of ultrasonic oscillations: superposition of longitudinal oscillations. Archive of Applied Mechanics. 2001;71:549-54. https://doi.org/10.1007/s004190100160
16. Liu W, Ni H, Wang P, Zhao B. Analytical investigation of the friction reduction performance of longitudinal vibration based on the modified elastoplastic contact model. Tribology International. 2020;146: 106237. https://doi.org/10.1016/j.triboint.2020.106237
17. Qu H, Zhou N, Guo W, Qu J. A model of friction reduction with in-plane high-frequency vibration. Proceedings of the Institution of Mechanical Engineers. Part J: Journal of Engineering Tribology. 2016;230(8):962-967. https://doi.org/10.1177/135065011562101
18. Sase N, Kurahashi T, Fujii M, Kutomi H, Fujii H. Control of friction coefficient between metal surfaces. Proceedings of the International Conference AMPT'97. 1997;2:609-615.
19. Storck H, Littmann W, Wallaschek J, Mracek M. The effect of friction reduction in presence of ultrasonic vibrations and its relevance to traveling wave ultrasonic motors. Ultrasonic. 2002;40:379-383. http://dx.doi.org/10.1016/S0041-624X(02)00126-9
20. Teidelt E, Starcevic J, Popov VL. Influence of ultrasonic oscillation on static and sliding friction. Tribology Letters. 2012;48:51-62. https://doi.org//10.1007/s11249-012-9937-4
21. Tsai CC, Tseng CH. The effect of friction reduction in presence of in-plane vibrations. Archive of Applied Mechanics. 2006;75:164-76. https://doi.org/10.1007/s00419-005-0427-0
22. Wang P, Ni H, Wang R, Li Z, Wang Y. Experimental investigation of the effect of in-plane vibrations on friction for different materials. Tribology International. 2016;99:237-247. https://doi.org/10.1016/j.triboint.2016.03.021
23. Wang P, Ni H, Wang R, Liu W, Lu S. Research on the mechanism of in-plane vibration on friction reduction. Materials. 2017;10(9):1-21. https://doi.org/10.3390/ma10091015
24. Yang CL, Wu CS, Shi L. Analysis of friction reduction effect due to ultrasonic vibration exerted in friction stir welding. Journal of Manufacturing Processes. 2018;35:118-126. https://doi.org/10.1016/j.jmapro.2018.07.025
25. Shao G, Li H, Zhan M. A Review on Ultrasonic-Assisted Forming: Mechanism, Model, and Process. Chinese Journal of Mechanical Engineering. 2021;34(1):99. https://doi.org/10.1186/s10033-021-00612-0
26. Chovdhury MA, Helali MM. The effect of frequency of vibration and humidity on the coefficient of friction. Tribology International. 2006; 39(9):958-962. https://doi.org/10.1016/j.triboint.2005.10.002
27. Chovdhury MA, Helali MM. The effect of amplitude of vibration on the coefficient of friction for different materials. Tribology International. 2008;41(4):307-314. https://doi.org/10.1016/j.triboint.2007.08.005
28. Hess DP, Soom A. Normal vibrations and friction under harmonic loads: part I – Hertzian contacts. Journal of Tribology. 1991;113(1): 80-86. https://doi.org/10.1115/1.2920607
29. Popov M, Popov VL, Popov NV. Reduction of friction by normal oscillations. I. Influence of contact stiffness. Friction. 2017;5(1):45-55. https://doi.org/10.1007/s40544-016-0136-4
30. Xinyu M, Popov VL, Stracevic J, Popov M. Reduction of friction by normal oscillations. II. In-plane system dynamics. Friction. 2017;5(2): 194-206. https://doi.org/10.1007/s40544-017-0146-x
31. Cheng Y, Zhu PZ, Li R. The influence of vertical vibration on nanoscale friction: a molecular dynamics simulation study. Crystals. 2018;8(3):129. https://doi.org/10.3390/cryst8030129
32. Dahl PR. A solid friction model. Technical Report TOR-158(3107-18), The Aerospace Corporation, El Segundo, CA. 1968.
33. Dahl PR. Solid friction damping of mechanical vibrations. AIAA Journal. 1976;14(12):1675-1682. https://doi.org/10.2514/3.61511
34. Dupont P, Armstrong B, Hayward V. Elasto-plastic friction model: contact compliance and stiction. Proceedings of the American Control Conference, Chicago, Illinois 2000. 2000:1072-1077. https://doi.org/10.1109/ACC.2000.876665
35. Dupont P, Hayward V, Armstrong B, Altpeter F. Single state elasto-plastic friction models. IEEE Transactions on Automatic Control. 2002;47(5):787-792. https://doi.org/10.1109/TAC.2002.1000274
36. Leus M, Gutowski P. The experimental analysis of the tangential stiffness of the flat contact joints. Modelling in Engineering. 2009; 6(37):185-192 [in Polish].

Acknowledgements: This research was funded in whole by the National Science Centre, Poland; Grant No. 2021/05/X/ST8/01244.

Mariusz Leus: https://orcid.org/0000-0002-1073-1734

Paweł Gutowski: https://orcid.org/0000-0002-0618-2357

Marta Rybkiewicz: https://orcid.org/0000-0002-6584-033X